2011 IEEE International Conference on Rehabilitation Robotics
Rehab Week Zurich, ETH Zurich Science City, Switzerland, June 29 - July 1, 2011

Design and Implementation of a Training Strategy in Chronic Stroke with an Arm Robotic Exoskeleton

Antonio Frisoli, Member, IEEE, Edoardo Sotgiu, Caterina Procopio, and Massimo Bergamasco
PERCRO, TeCIP
Scuola Superiore Sant'Anna
Pisa-Italy

Bruno Rossi, MD, Carmelo Chisari, MD
Neurorehabilitation Unit, Department of Neurosciences,
University of Pisa
Pisa-Italy

Abstract—**The distinguishing features of active exoskeletons are the capability of guiding arm movement at the level of the full kinematic chain of the human arm, and training full 3D spatial movements. We have specifically developed a PD sliding mode control for upper limb rehabilitation with gain scheduling for providing "assistance as needed", according to the force capability of the patient, and an automatic measurement of the impaired arm joint torques, to evaluate the hypertonia associated to the movement during the execution of the training exercise. Two different training tasks in Virtual Reality were devised, that make use of the above control, and allow to make a performance based evaluation of patient's motor status. The PERCRO L-Exos (Light-Exoskeleton) was used to evaluate the proposed algorithms and training exercises in two clinical case studies of patients with chronic stroke, that performed 6 weeks of robotic assisted training. Clinical evaluation (Fugl-Meyer Scale, Modified Ashworth Scale, Bimanual Activity Test) was conducted before and after treatment and compared to the scores and the quantitative indices, such as task time, position/joint error and resistance torques, associated to the training exercises.**

Keywords-component; Robotic Rehabilitation, Arm Exoskeleton, Chronic Stroke Patient

I. INTRODUCTION

REDUCING the impact of stroke on the usual daily activities of elderly patients has been becoming a primary objective in developed countries. Rehabilitation plays a fundamental role in reducing the residual motor deficits of stroke patients, both during (acute/subacute phase) and after (chronic phase) hospitalization. In the last decade research studies have focused both on the development of novel robotic interfaces and on the use of Virtual Reality technologies for neurorehabilitation [1].

Well-established traditional stroke rehabilitation techniques rely on thorough and constant exercise [2, 3], which patients are required to carry out already during in-patient hospital care with the help of therapists, as well as during daily life at home. Early initiation of active movements by means of repetitive training has proved its efficacy in guaranteeing a good recovery of motor capability [4].

The use of robot devices in rehabilitation can provide high intensity, repetitive, task specific and interactive treatment of the impaired upper limb and an objective, reliable mean of monitoring patients progress. Systematic reviews confirm the potential for robotic assisted devices to elicit improvements in upper limb function [5, 6].

It has been recently shown that robotic assisted therapy is equivalent to high intensive manual therapy in terms of comparable results in the recovery of stroke [7]. Moreover, there is evidence that training performed in Virtual Reality can induce cortical reorganization and associated recovery in chronic stroke [8, 9], and that also training performed with passive devices in a gravity-reduced environment can provide comparable results to those achieved with robotic assisted rehabilitation [10].

On the other hand, several studies ([11, 12]) have demonstrated positive effects of Virtual Reality on rehabilitation, which enhances cognitive and executive functions of stroke patients by allowing them to receive enhanced feedback on the outcome of the rehabilitation tasks he/she is performing. Moreover, VR can provide an even more stimulating videogame-like rehabilitation environment when integrated with force feedback devices, thus enhancing the quality of the rehabilitation.

While several studies have already investigated the effects of robot assisted training in planar movements performed in the horizontal plane [13], the effect of training on the control and production of multi-joint and spatial functional arm movements, including movements against gravity, in hemiparetic subjects has received less attention.

There are proofs in literature that gravity compensation leads to a recovery of motor abilities. The first study demonstrated that individuals with chronic stroke whose arm function is compromised in a normal gravity environment can perform reaching and drawing movements with gravity compensation [14]. It has been demonstrated that exercising the affected arm over an eight week period improved unassisted movement ability.

Upper limb exoskeleton systems present unique features for upper limb rehabilitation: first the possibility of controlling the full arm posture by selective joint control, second the possibility of performing large three-dimensional movement and third providing a good compensation for the impaired arm's weight, by applying gravity support forces at more

contact points, i.e. at the level of humerus and radius/ulna segments.

Several arm rehabilitation robotic exoskeleton devices have been developed in the last 10 years. Some examples include the ARMin-II [15], the Salford Exoskeleton [16], and the L-Exos[17], that was used in this study.

The aim of this work is to introduce new strategies for using in a more efficient way active exoskeleton systems in upper limb neurorehabilitation. We introduce a new control scheme based on a gain scheduling and PID sliding mode, that can implement an "assistance as needed" training strategy, and two VR based exercises that can specifically train movements in the vertical and sagittal plane. Some automatic performance measurements are defined and associated to the training exercises, and the relation of the above performance measurements is shown in comparison with clinical indexes.

II. SYSTEM DESCRIPTION

The rehabilitation platform (Figure 1) is composed of the the light exoskeleton robotic device (L-exos) mounted on a mobile support of device, a control system and a graphic workstation with associated display.

The L-Exos is a force feedback exoskeleton for Upper Limb Rehabilitation (ULR) of right-handed patients. It is characterized by a serial open kinematics with five degree-of-freedom (DoF), as shown in Figure 2.a, and capable of providing force–feedback through the first four active DoFs. The exoskeleton pose is measured by four digital encoders associated with the corresponding human arm joints, shoulder adduction/abduction, flexion/extension and internal/external rotation and forearm flexion/extension ($\mathbf{q} = \{q_1, q_2, q_3, q_4 \in \mathbb{R}\}$) and a fifth passive joint corresponding to the wrist pronation/supination. Through those measurements the equivalent pose of the human arm wearing the exoskeleton can be identified.

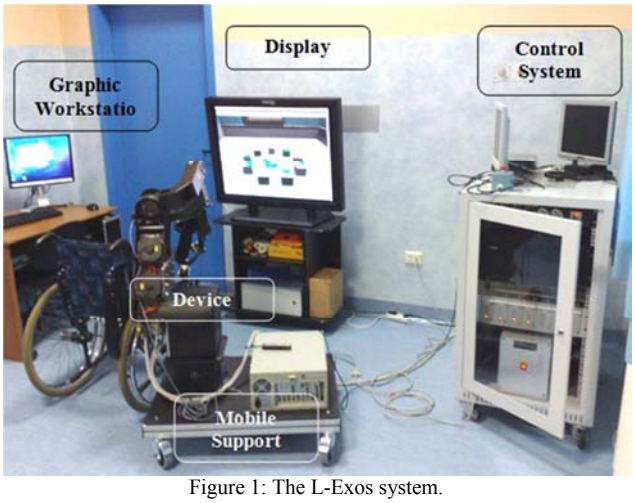

Figure 1: The L-Exos system.

The device is capable to exert a controlled maximum force up to 100N on the hand palm of the patient oriented along any direction, within the space reachable by the device.

The position accuracy expressed at the end-effector is less than 1 mm, equivalent to 0.05° expressed in the joint space.

In order to have a direct measurement of the force exerted by the patient during the training and evaluation trials, a tri-axial force sensor was specifically developed and embedded in the handle. In addition pressure sensors were glued on the handle surface (Figure 2.b) to detect the grasping force exerted on the handle.

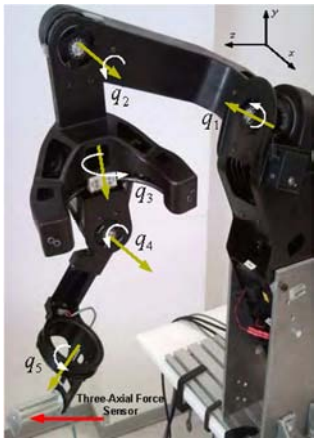

(a)

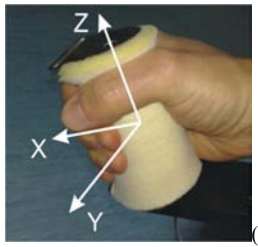

(b)

Figure 2: L-exos kinematics (a) and the sensorized handle (b).

III. DESIGN OF THE CONTROL FOR ACTIVE ULR EXOSKELETONS

The main principles underlying the development of the proposed controller were:

1. to guarantee a finite time convergence and a safe active guidance notwithstanding user's behavior;
2. to adaptively modulate the gains of the control law of the robot assistance, according to the user's performance;
3. to deal with holonomic constraints, introduced to guide the movement along pre-defined trajectory, e.g. a line;
4. to compute the arm pose associated to the end-effector position by an inverse kinematics algorithm, taking into account the redundancy of the overall system;

Considering points 1 and 2, a nonlinear controller was developed in order to be fast and robust against parametric and unknown perturbations, based on a non-linear PID sliding control derived from [18].

In Figure 3 it is reported the general architecture of the control algorithm for active assistance of motion. Such an architecture is composed of:

- a Motion Planner, that generates the path in the Cartesian space to be followed by the patient;
- a Virtual Constraints Planner, that defines the virtual constraints imposed to the patient movement;
- the Sliding PD Controller, that computes the required robot torques;
- the Gain Scheduler, to modulate the control gains on the base of the force exerted by the patient.

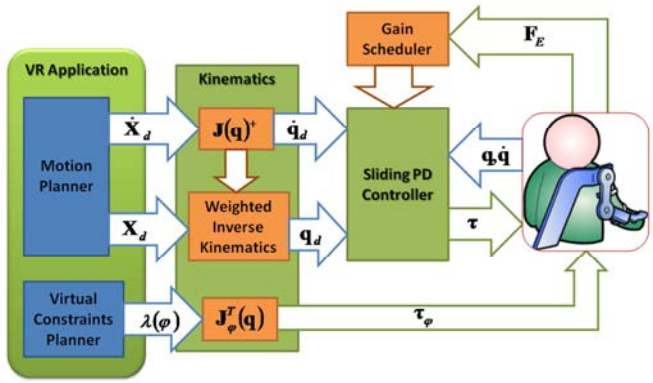

Figure 3: The general blocks of interconnection between the hardware and the software control.

A. A sliding mode PD control for upper limb rehabilitation

The design of the PD sliding mode control was based on the following assumptions. Consider the following dynamic equation for the full system:

$$\mathbf{H}(\mathbf{q})\ddot{\mathbf{q}} + \mathbf{C}(\mathbf{q},\dot{\mathbf{q}})\dot{\mathbf{q}} + \mathbf{G}(\mathbf{q}) + \mathbf{B_0}\dot{\mathbf{q}} + \mathbf{C_0}\text{sign}(\dot{\mathbf{q}}) = \boldsymbol{\tau} - \mathbf{J}^{\mathbf{T}}\mathbf{F_E}$$

where **H** and **C** represent the matrices associated to the Inertia and Coriolis terms of robot dynamics respectively, **G** is the gravity term, $\mathbf{B_0}$ the intrinsic system viscosity and $\mathbf{C_0}$ models the friction. The matrix **J** is the Jacobian, that maps the force at the end effector $\mathbf{F}_E$ in the joint torques $\boldsymbol{\tau}$.

Let us consider to have a reference desired joint position to follow, that is imposed to the patient from the Motion Planning algorithm. The joints and speed joints error are:

$$\Delta\mathbf{q} = \mathbf{q} - \mathbf{q_d}$$

$$\Delta\dot{\mathbf{q}} = \dot{\mathbf{q}} - \dot{\mathbf{q}}_\mathbf{d} .$$

The control law adopted is a PD second-order sliding mode control given by

$$\boldsymbol{\tau} = -\mathbf{K}_d\mathbf{S} ,$$

where the diagonal definite positive matrix $\mathbf{K}_d$ is defined as a positive feedback gain, and **S** is the extended error whose the nominal manifold sliding surface is defined as

$$\mathbf{S} = \mathbf{S_C} + \boldsymbol{\gamma}\int_{t_0}^{t} tanh\big(\mathbf{S}_C(\lambda)\big)d\lambda ,$$

where $\mathbf{S_c}$ is defined as follows:

$$\mathbf{S}_C = \mathbf{S}_p - \mathbf{S}_0 ,$$

with

$$\mathbf{S}_p = \Delta\dot{\mathbf{q}} + m\Delta\mathbf{q} ,$$

$$\mathbf{S}_0 = \mathbf{S}_p(t_0)e^{-\rho_0(t-t_0)} .$$

The control parameters in the above formula have the following meaning:

- *m* provides the slope of the convergence of error at zero, as shown in Figure 4, where it is possible to see how the error at infinity is constrained to converge to zero ($\mathbf{S}_C = 0$) in the error phase space along a line with slope *m*.
- γ, introduces the second order sliding mode responsible of the tracking along the sliding surface;
- ρ_0 and t_0 parameters allow to smooth the starting phase.

The sliding model control guarantees the properties of convergence of error, limiting minimum time and maximum forces generated by the impedance control.

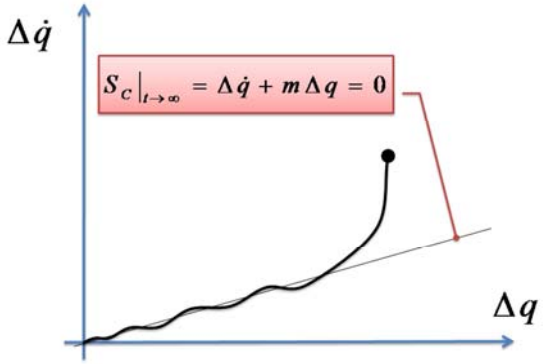

Figure 4: Phase plane trajectory of the system: basic representation of the finite time convergence of the sliding mode control.

With some algebraic manipulation, it is easy to show that the same control can be demonstrated to be equivalent to the following one [19]:

$$\boldsymbol{\tau} = -\mathbf{K}_d\Delta\dot{\mathbf{q}} - \mathbf{K}_d m\Delta\mathbf{q} + \mathbf{K}_d\mathbf{S}_0 - \mathbf{K}_d\gamma\int_{t_0}^{t} tanh\big(\mathbf{S}_C(\lambda)\big)\,d\lambda ,$$

that can be alternatively formulated as a PD control scheme plus a second-order sliding mode term:

$$\boldsymbol{\tau} = \underbrace{-\mathbf{K}_p\Delta\mathbf{q} - \mathbf{K}_d\Delta\dot{\mathbf{q}}}_{\text{PD Control}} + \underbrace{\mathbf{K}_d\mathbf{S}_0 - \mathbf{K}_d\gamma\int_{t_0}^{t} tanh\big(\mathbf{S}_C(\lambda)\big)\,d\lambda}_{\text{Second-Order Sliding Mode}}$$

A comparison of the above expressions allows to quickly conclude that the control gain $\mathbf{K}_p$ (representing the impedance value) is proportional to $\mathbf{K}_d$, if *m* is a constant positive parameter:

$$\mathbf{K}_p = m\mathbf{K}_d$$

1) Gain scheduling control

The parameter $\mathbf{K}_d$ represents a robust way to modulate the impedance displayed to the patient. We decide to adjust its value on-line according to the user's intention of movement, measured through the force sensor at the handle. The parameter $\mathbf{K}_d$ is set as a function of the exerted force of the user, depending on the interaction force through an exponential function with "time" constant expressed by a specific parameter τ, with the control law:

$$\mathbf{K}_d = \mathbf{K}_{d,max}\big(e^{-\tau\|\mathbf{F_t}\|}\big),$$

where $\mathbf{K}_{d,max}$ represents the maximum allowable gain parameter.

Please note, that $\|\mathbf{F_t}\|$ is the absolute value of the component of force in the direction of the desired motion, e.g. along a line if the patient is performing a rectilinear guided motion.

These two parameters, τ and $\mathbf{K}_{d,max}$, can be set directly by the therapist by means of a GUI, to tune up the controller according to the patient requirements. The global effect of this gain scheduling control scheme is that the patient will perceive an impedance that is varying according to his/her performance. When the patient is exerting a resistance force (due to spasticity) or an active force (due to his/her ability to execute the movement), the robot will gradually reduce the gain to reduce the amount of force exchanged with the patient.

2) Virtual constraints

It also possible to add a virtual constraint of motion along a line. This kind of constraint, such as the one shown in Figure 5, can be analytically expressed as the linear combination of two implicit linear functions defining the two constraint planes:

$$\varphi(\mathbf{p}) = 0 : \begin{cases} \varphi_1(x,y,z) = 0 \\ \varphi_2(x,y,z) = 0 \end{cases}$$

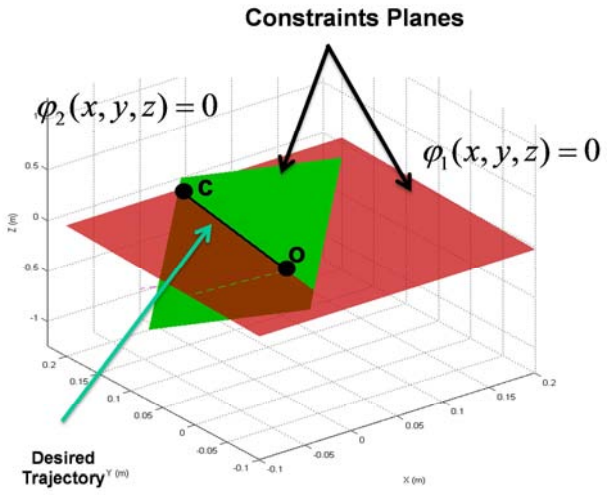

Figure 5 Example of motion constrained along a line.

Making the derivative of the above equations produces a constrained Jacobian matrix J_φ with dimension 2x4, such that

$$\frac{\partial \varphi(\mathbf{p})}{\partial \mathbf{p}} \mathbf{J}(\mathbf{q})\dot{\mathbf{q}} = \mathbf{J}_\varphi(\mathbf{q})\dot{\mathbf{q}} = \mathbf{0}\,.$$

If we introduce a vector $\boldsymbol{\lambda} = (\lambda_1, \lambda_2)$, associated to the implicit functions as follows $\lambda_i = m_i(\ddot{\varphi}_i) + b_i(\dot{\varphi}_i) + k_i(\varphi_i)$, where φ_i represents the error when the virtual constraint is not verified, and m_i, b_i and k_i are positive parameters to be adjusted to define a critically damped dynamic system. In this way the virtual constraint can be implemented in the control algorithm by the additional term $\mathbf{J}_\varphi{}^T\boldsymbol{\lambda}$:

$$\begin{cases} \mathbf{H}(\mathbf{q})\ddot{\mathbf{q}} + \mathbf{C}(\mathbf{q},\dot{\mathbf{q}})\dot{\mathbf{q}} + \mathbf{G}(\mathbf{q}) + \mathbf{B_0}\dot{\mathbf{q}} + \mathbf{C_0}\mathrm{sign}(\dot{\mathbf{q}}) = \boldsymbol{\tau} - \mathbf{J}^T\mathbf{F_E} + \mathbf{J}_\varphi{}^T\boldsymbol{\lambda} \\ \varphi(\mathbf{q}) = 0 \end{cases}$$

B. Selective joint control

Due to the higher number of DoFs of the exoskeleton than the number of DoFs of operational space (4 vs. 3), the system is task redundant. In this case the Jacobian matrix, that describes a linear mapping between joint velocity space and the end-effector space, is not square and cannot be inverted.

A right weighted pseudo-inverse $\mathbf{J}^\dagger$ of the Jacobian matrix can be defined to invert the equation $\Delta\mathbf{X} = \mathbf{J}\Delta\mathbf{q}$, by finding the inverse mapping $\mathbf{J}^\dagger$ that minimizes the function $\mathbf{q}^T\mathbf{W}\mathbf{q}$, where $\mathbf{W}$ is a diagonal matrix of weights that penalizes the movement of specific joints:

$$\mathbf{J}(\mathbf{q})^\dagger = \mathbf{W}^{-1}\mathbf{J}(\mathbf{q})^T(\mathbf{J}(\mathbf{q})\mathbf{W}^{-1}\mathbf{J}(\mathbf{q})^T)^{-1}.$$

This weighted pseudo-inverse is then in the numerical integration algorithm for inverting the direct kinematics, as follows:

$$\Delta\mathbf{q}_d = \mathbf{J}(\mathbf{q})^\dagger\Delta\mathbf{X}_d$$

$$\mathbf{q}_{i+1} = \mathbf{q}_i + \Delta\mathbf{q}_d.$$

Where $\mathbf{X}_d$ and $\mathbf{q}_d$ represent the desired Cartesian and joint trajectory.

The above formulation was adopted to convert a desired trajectory expressed in the Cartesian space in an equivalent one expressed in joint space.

C. High level control strategies

Based on the above formulation two different high level control strategies were implemented for movement training, respectively for guided and free motion:

•Guided motion

-Passive Mode (impedance control): the patient is passively guided by the robot along the trajectory to be executed (trajectory tracking, reaching objects) with force proportional to the error;

- Gain Scheduling Position Mode: the amount of the robot action on the patient is regulated by the force measured at the exoskeleton handle. If the patient does not exercise forces (meaning he is not able to follow the moving reference), he is assisted by the robot to reduce the error. Otherwise, assist gain is gradually reduced to let the patient free to follow the reference trajectory;

•Free Motion

-Direct Force Mode and Counterbalancing assistance: this option lets the patient free to interact with the virtual environment providing only a counterbalancing of weight of his own arm.

In the guided modality, there is the possibility of selecting a different control strategy among the 2 directions of space:

- Longitudinal direction (gain schedule control triggered by force input or impedance control)
- Transversal directions (impedance control determined by implicit geometric constraints)

IV. THE TRAINING SCENARIOS

Two main training exercises were designed for the recovery of function in tasks of reaching objects in frontal, ipsilateral and contralateral parts of the workspace.

1) REACHING:

The environment consists of a virtual room with 3 libraries each containing fixed objects, arranged horizontally on its shelves, as shown in Figure 6: a central library containing 3 different objects (two glasses and a cup),two lateral libraries containing 2 objects (glasses). The 7 objects are the targets of reaching movements. The patient hand is represented in the virtual environment as a bottle (avatar). The parameters (environmental and control parameters), which can be varied to adapt the work sessions on the type of patient and his/her hemiplegia severity, are: the position of the shelf, number of repetition, velocity of execution. The control operational modalities of the device define differently control strategies of the joint position of the exoskeleton: Passive or Gain Scheduling Position mode.

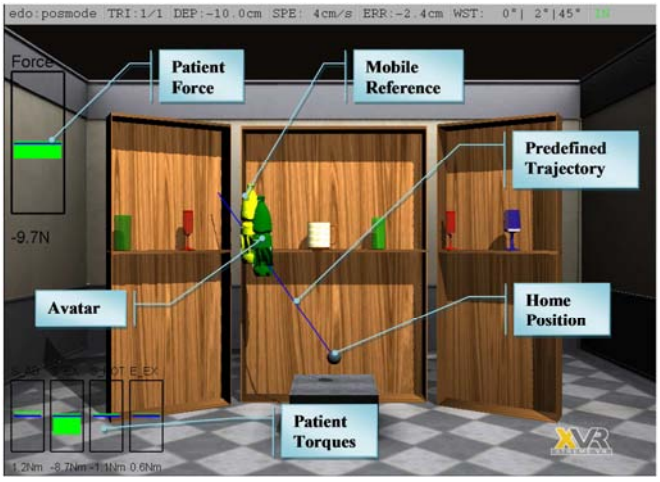

Figure 6: Virtual environment of Reaching Task.

The gain scheduling assistance impedance control was developed since:

- it allows the patient to initiate the movement without any robotic guidance;
- this form of triggered assistance encourages patient self-initiated movement, which is thought to be essential for motor learning.

As far as the training scenarios, the reaching task is broke down in the following phases (Figure 7):

1) the patient is asked to pronosupinate hand in order to reach a comfortable position. Patients recovering from stroke are normally asked to find a comfortable position for their wrist;

2) Motion start with inward movement: in this phase, normally contraction leads to exhibit a resistance by most of the patients;

3) Pronosupination to align to the target bottle and pouring water in the glass (yellow one, in Figure 6);

4) Inward motion with return to the start position.

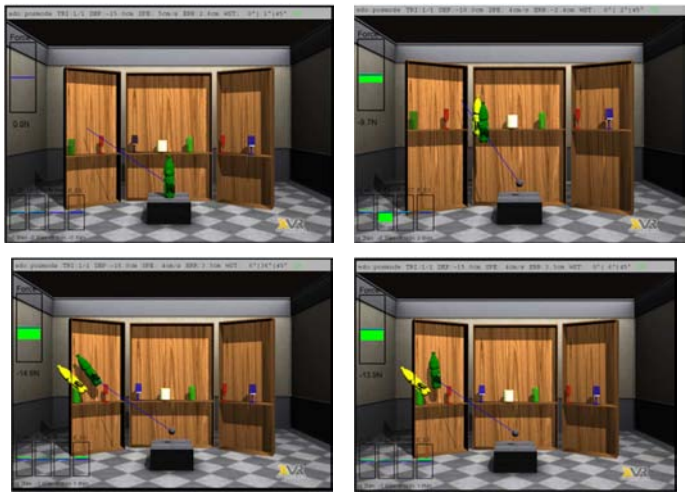

Figure 7: Sequence of phases in the execution of the exercise.

Since the trajectory is defined a priori, the patient's arm is guided actively at the level of shoulder and elbow joints. This makes possible to estimate the resistance torques exerted by the patient at the level of shoulder and elbow joints: they are displayed on the screen as a bar plot, so that the therapist can verify at each time the level of contraction induced by hypertonia, and adjust the difficulty of the exercise accordingly to it (see bars in the bottom left panel of Figure 6).

2) CUBES:

The environment shows several blocks placed around a circle on a vertical wall. The patient should move the arm in the vertical plane and back/forward to grasp blocks and place them at the right place.

Figure 8: The virtual puzzle task.

Through the pressure sensors mounted on the handle, the patient can modulate the needed grasping force. Some patients, that are unable to exert grasping, wore a passive orthosis on their own hand. At the end of each training session performance time achieved in previous and current sessions are shown to the patient.

Difficulty of sessions is tailored to the patient's ability and performance. An evaluation session follows at the end of each session requiring the patient to move blocks disposed symmetrically among 12 radial directions from periphery to center and the opposite, as shown in Figure 9. Both time to

move each block and trajectories were recorded in each evaluation session.

The only facilitation of movement provided through the robot in this scenario was the gravity compensation of the impaired limb.

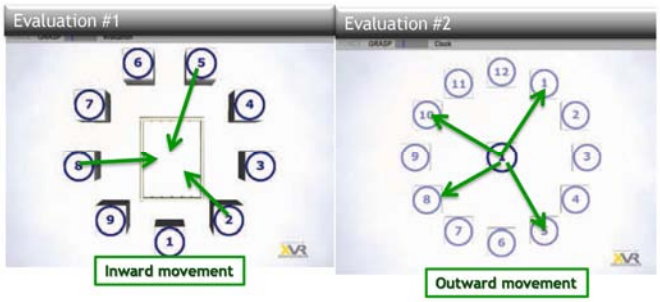

Figure 9 The evaluation session

V. PRELIMINARY CLINICAL EVALUATION

To assess the goodness and usability of the proposed training strategy, two chronic stroke patients were asked to use the system for a training period of 6 weeks, three times per week. Patients were evaluated before and after the training with Fugl-Meyer Scale for upper limb, Modified Ashworth Scale and Bimanual Activity Test for functional assessment.

A. Patients baseline data

As shown from Table 1, the two patients presented respectively a severe and moderate impairment, as denoted by FMA values. Patient 1 denoted also a relevant hypertonia, that was completely absent in the second. From the bimanual activity scale, we measured the mean time in the execution of ADL tasks, that was lower for patient 2 according to a ratio 4:3 to average time of patient 1.

TABLE 1 PATIENTS BASELINE DATA

Patient	Age	Sex	FMA	MAS	Bimanual Activity Test	
					time	quality
P1	61	M	19	12	19,36	1,91
P2	79	M	41	0	15,84	2,95

The training scenario needed to be adapted to the patients according to their specific needs.

B. Impedance assistance vs. assist as needed

Only patient P2 was able to use the gain scheduled assistance modality of the controller in the first scenario. We can see in the bar plot of Figure 10 how there is no change in the longitudinal force in the inward movement, where the flexor synergy is normally adopted by the patient. It is interesting to note that in the outward phase, the force exerted by the subject to perform the movement is on average less in the gain scheduled modality, confirming the hypothesis that this control modality reduces the effort required to the patient to perform the movement.

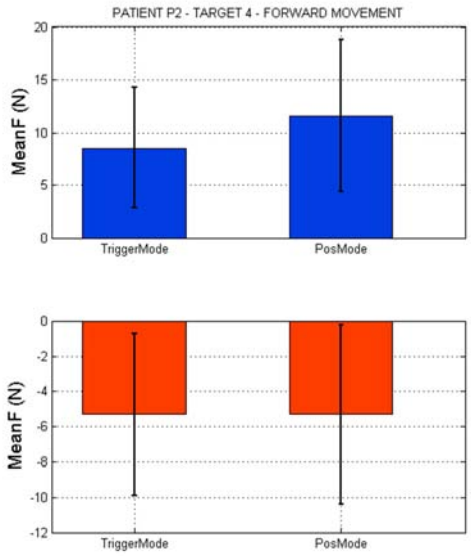

Figure 10: Comparison of force exerted at the handle during the modalities of triggered with gain schedule (left) and classical impedance control (right). Blue line represent outward movement, while red line inward movement.

C. Joint Torque

In patient 2, joint torques were continuously monitored over sessions to assess the increment of spasticity. In the bar plot about joint 2 (Figure 11) we can see clearly how the muscles recruited at the shoulder level for the extension movement reduce their tone as an effect of the treatment. This validates the correctness of the performed exercise.

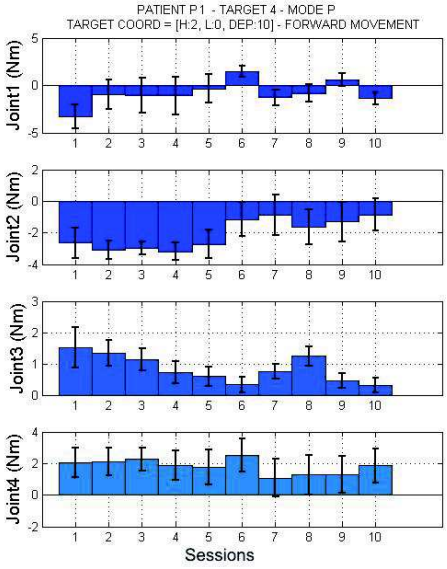

Figure 11: Joint torques as a function of session (joint 2 represents the flexion/extension of shoulder).

D. Performance-based evaluation

It is interesting to see how performance can be easily represented in terms of polar plots (see diagram in Figure 12 for patient 1), where time required to move respectively inward and outward is shown for different directions, symmetrical disposed at intervals of 30 deg, around a circle

oriented in the vertical plane. The effect of treatment is represented by an improvement in terms of velocity, and so of time reduction, associated to the execution of the movement. It should be noted that directions 2 and 3 in the polar diagram, where the worst performance is observed, are directions in which the highest counterbalance of the arm's weight is required for the exploration of the ipsilateral part of the workspace.

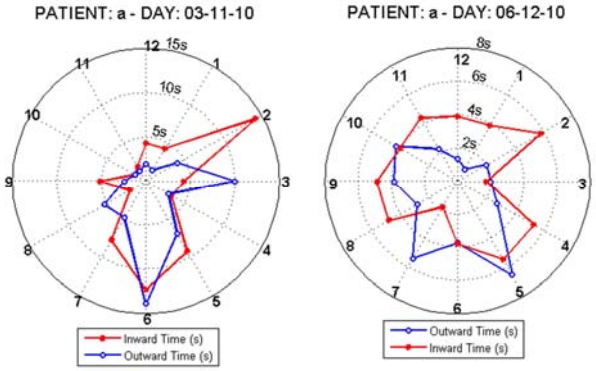

Figure 12: Time requested to move outward (blue) and inward(red) before and after training for patient 1.

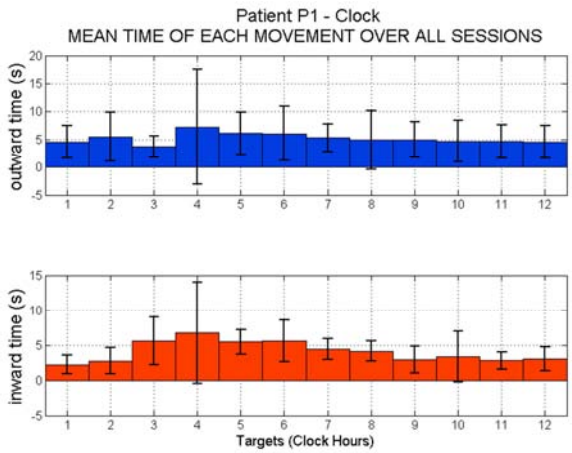

Figure 13: Mean time in the outward (blue) and inward (red) phase distributed along the 12 angular sectors for patient 1.

In Figure 13 it is reported the mean time distribution averaged across all therapy sessions, that show how the worst performance is achieved in terms of higher time and variability of performance for targets located in the ipsilateral workspace.

We report in Figure 14, the trend of reduction of total time required to move toward and backward the twelve targets over the number of sessions for the two patients (the higher number of sessions of patient 2 is due to higher number of repetitions he has executed during each therapy sessions than patient 1). It is interesting to note that a relative proportion among times is maintained, with results very similar to the performance observed in the Bimanual Activity Scale.

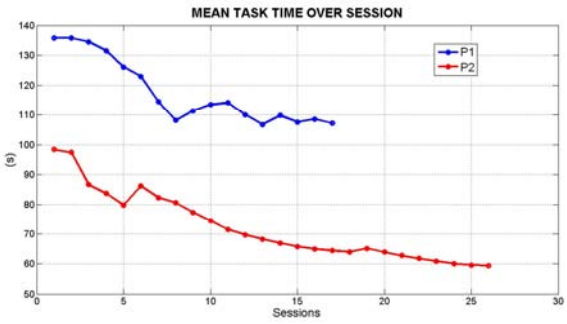

Figure 14 Overall time decrement vs. number of sessions for patient 1 and 2

Following the T-angle measurement introduced in [20], it is possible to have an estimate of the smoothness of movement performed by the patient. For sake of explanation we report in Figure 15 the two plots of angular elbow speed vs. elbow excursion obtained during the reaching of target 3. It is possible to see how the number of encirclements and cuspidal points is reduced after training, indicating a movement performed with a smoother profile.

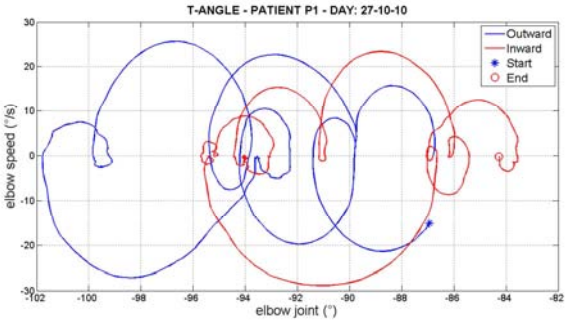

(a) Pre-training, T-angle plot for target 3, patient P1

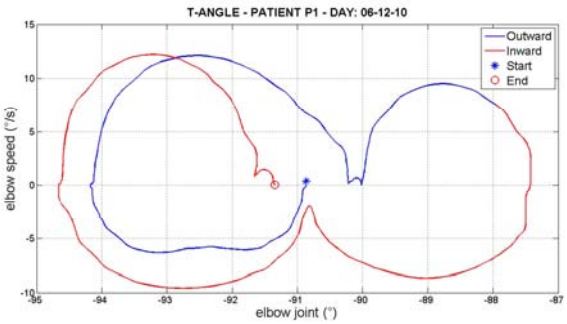

(a) Post-training, T-angle plot for target 3, patient P1

Figure 15 Plot of T-angle relative to elbow excursion measured through the exoskeleton (x axis elbow excursion(deg), y axis speed of elbow excursion (deg\sec)

E. Clinical evaluation

After training, the Fugl-Meyer, Mas scale and Bimanual Activity tests were evaluated and their values are reported in Table 2.

It is interesting to note how we observe a modification of time in the bimanual activity scale coherent with the experimental observation reported in Figure 14. This may represent a good

indication of transfer of learning from the virtual reality to the real setting.
Overall spasticity is decreased in the two subjects and FMA is increased of several points.

Table 2 PATIENT EVALUATION AT DISCHARGE.

Patient	FMA	MAS	Bimanual Activity Test	
			time	quality
P1	22	5	3,58	3,58
P2	47	-3	11,73	3,58

VI. DISCUSSION AND CONCLUSIONS

The above results show that performance indices associated to the training exercises are indicative of changes observed with the clinical evaluation.
The design of the training strategy allows to tailor the robot control to patient's needs, so that it is possible to focus on the reduction of hypertonia on patients with higher spasticity, or on the coordination of movement in the patients with overall better sensorimotor recovery.

VII. ACKNOWLEDGEMENTS

This work was partially supported under the projects SKILLS, and BRAVO, respectively funded by the EU (ICT Program) and the Italian Institute of Technology (Seed Program). A special thanks goes to Dr. Luis Ivan Lugo-Villeda, that made a substantial contribution to the ideation of the presented PD sliding mode controller. Sadly he suddenly and unexpectedly passed away at time of writing of this work.

REFERENCES

[1] G. Prange, M. Jannink, C. Groothuis-Oudshoorn, *et al.*, "Systematic review of the effect of robot-aided therapy on recovery of the hemiparetic arm after stroke," *Journal of Rehabilitation Research and Development,* vol. 43, p. 171, 2006.

[2] L. Diller, "Poststroke Rehabilitation Practice Guidelines," *International Handbook of Neuropsychological Rehabilitation,* 2000.

[3] J. H. van der Lee, R. C. Wagenaar, G. J. Lankhorst, *et al.* (1999). *Forced Use of the Upper Extremity in Chronic Stroke Patients Results From a Single-Blind Randomized Clinical Trial*.

[4] C. Butefisch, H. Hummelsheim, P. Denzler, *et al.*, "Repetitive training of isolated movements improves the outcome of motor rehabilitation of the centrally paretic hand.," *J Neurol Sci,* vol. 130, pp. 59-68, 1995.

[5] A. A. Timmermans, H. A. Seelen, R. D. Willmann, *et al.*, "Technology-assisted training of arm-hand skills in stroke: concepts on reacquisition of motor control and therapist guidelines for rehabilitation technology design," *J Neuroeng Rehabil,* vol. 6, pp. 1-18, 2009.

[6] N. B. Ruth, B. Sandra, and C. Richard, "Training-induced changes in the pattern of triceps to biceps activation during reaching tasks after chronic and severe stroke," *Experimental Brain Research,* vol. 196, pp. 483-496, 2009.

[7] A. C. Lo, P. D. Guarino, L. G. Richards, *et al.*, "Robot-assisted therapy for long-term upper-limb impairment after stroke," *New England Journal of Medicine,* 2010 2010.

[8] S. H. You, S. H. Jang, Y. H. Kim, *et al.*, "Virtual reality-induced cortical reorganization and associated locomotor recovery in chronic stroke: an experimenter-blind randomized study," *Stroke,* vol. 36, p. 1166, 2005.

[9] A. Frisoli, A. Montagner, L. Borelli, *et al.*, "Arm rehabilitation with a robotic exoskeleton in virtual reality," in *ICORR 2007*, 2007, pp. 631–642.

[10] R. J. Sanchez, J. Liu, S. Rao, *et al.*, "Automating arm movement training following severe stroke: functional exercises with quantitative feedback in a gravity-reduced environment," *Neural Systems and Rehabilitation Engineering, IEEE Transactions on,* vol. 14, pp. 378-389, 2006.

[11] L. Hodges, P. Anderson, G. Burdea, *et al.*, "Treating psychological and physical disorders with VR," *IEEE Computer Graphics and Applications,* pp. 25-33, 2001.

[12] D. Jack, R. Boian, A. Merians, *et al.*, "Virtual reality-enhanced stroke rehabilitation," *Neural Systems and Rehabilitation Engineering, IEEE Transactions on,* vol. 9, pp. 308-318, 2002.

[13] M. Ferraro, J. Palazzolo, J. Krol, *et al.*, "Robot-aided sensorimotor arm training improves outcome in patients with chronic stroke," *Neurology,* vol. 61, p. 1604, 2003.

[14] R. Sanchez, J. Liu, S. Rao, *et al.*, "Automating arm movement training following severe stroke: functional exercises with quantitative feedback in a gravity-reduced environment," *Neural Systems and Rehabilitation Engineering, IEEE Transactions on,* vol. 14, pp. 378-389, 2006.

[15] T. Nef, M. Mihelj, G. Kiefer, *et al.*, "ARMin-exoskeleton for arm therapy in stroke patients," 2008, pp. 68-74.

[16] N. Tsagarakis and D. Caldwell, "Development and control of a 'soft-actuated'exoskeleton for use in physiotherapy and training," *Autonomous Robots,* vol. 15, pp. 21-33, 2003.

[17] A. Frisoli, F. Salsedo, M. Bergamasco, *et al.*, "A force-feedback exoskeleton for upper-limb rehabilitation in virtual reality," *Applied Bionics and Biomechanics,* vol. 6, pp. 115-126, 2009.

[18] V. Parra-Vega, S. Arimoto, Y. Liu, *et al.*, "Dynamic sliding PID control for tracking of robot manipulators: theory and experiments," *Robotics and Automation, IEEE Transactions on,* vol. 19, pp. 967-976, 2004.

[19] L. Lugo-Villeda, A. Frisoli, O. Sandoval-Gonzalez, *et al.*, "Haptic guidance of Light-Exoskeleton for arm-rehabilitation tasks," in *Robot and Human Interactive Communication RO-MAN 2009, The 18th IEEE International Symposium on* 2009, pp. 903-908.

[20] M. C. Cirstea, A. B. Mitnitski, A. G. Feldman, *et al.*, "Interjoint coordination dynamics during reaching in stroke," *Exp Brain Res,* vol. 151, pp. 289-300, Aug 2003.